International Scholarly Research Network
ISRN Materials Science
Volume 2011, Article ID 784615, 5 pages
doi:10.5402/2011/784615

Research Article

Liquid Crystal-Based Reconfigurable Tunable Filter with DBR Topology

S. Missaoui and M. Kaddour

Electronics Laboratory, Department of Physics, Faculty of Science, University of Tunis El Manar, Rommana 1068, Tunisia

Correspondence should be addressed to S. Missaoui, sayed.elmissaoui@gmail.com

Received 25 June 2011; Accepted 2 August 2011

Academic Editor: S. Furumi

The use of liquid crystals for tunable filter in planar technology is proposed. The design is based on a dual-behavior resonator (DBR) topology. These resonators are based on the association of different parallel open-ended stubs and allow the designer to independently control the in-band and out-of-band responses of the filter. To benefit from liquid crystal anisotropy and thus obtain agility, a bias voltage is applied. The simulated results are compared with measured data, and good agreement is obtained.

1. Introduction

The demand on tunable or reconfigurable components at micro- and millimeter waves increased during the last years. Today, these difficult problems are the subject of intensive studies in microwave planar filters [1–5]. For such applications, the use of dual-behavior resonators (DBRs) [1, 2] appears as a quite convenient solution because they allow the control of two attenuated bands on either side of one bandpass [1]. The agile microwaves devices [6–10] permit a compensation of the technological scatterings, the improvement of the instrumentation and the increase of the integration functions. The agile filters for example, present in the useful loads represent an important proportion so much in weight that in volume of the embarked facilities. Indeed, the extremely stern constraints imposed by the systémiers (in terms of selectivity, losses, rejection, baldness, attenuation of the parasitic ascents, etc.) lead today the inventors to move toward solutions of type accordable waves guides that to replace the stationary components by variable components. The variable components can be conceived using semiconductors, MEMS, ferrites, or ferroelectrics. One of the sought properties for this device is the possibility of external control. For decades, to achieve this objective, enormous efforts have been deployed for using new materials that have a better functionality. Among these materials, liquid crystals (LCs) are potentially useful. LC state is known to vary with temperature from solid to liquid. The nematic phase corresponds to the state where molecules have an orientational order, but no positional one. Application of an electric field to LC changes the direction of molecules and may create significant anisotropy, which explains why LC is currently chosen for microwave applications. This anisotropy varies with frequency and temperature [11].

This paper propose device using planar technology-based on LC materials. This choice allows the LC anisotropy property to the excited radio frequency field [12, 13] polarization with an electrostatic field. Numerical results for design filter with an LC cavity are compared with the existing data to confirm the accuracy of the proposed analysis.

2. Properties of Liquid Crystals

LCs are attractive substrates for microwave devices. They possess a significant tuneable dielectric constant in the microwave band, which can be exploited in compact and reconfigurable devices such as phase shifters, antennas, and filters. When designing such devices two main problems are normally encountered. Depending on the temperature, liquid crystal phase exists in a mesophase between a crystalline solid and an isotropic liquid [5] as shown in Figure 1. In this state, the material can flow like a liquid but at the same time molecules have orientational order. The size of the molecule is typically a few nanometers. This shape anisotropy causes

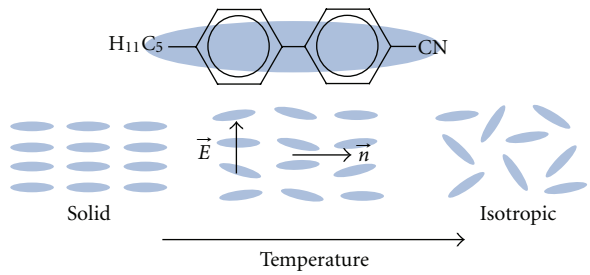

Figure 1: Schematic of a typical LC molecule (K15) and its temperature dependency.

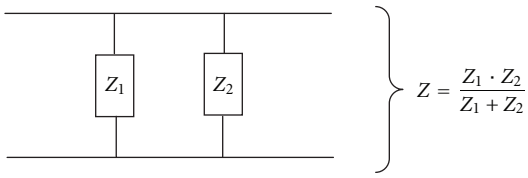

Figure 2: DBR, the basic resonant structure.

anisotropy in terms of the dielectric constant, as will be described in Figure 1.

In an aligned nematic liquid crystal, linearly polarized light incident as an extraordinary wave will see a permittivity ε_{LC} given by [14]

$$\varepsilon_{LC} = \frac{\varepsilon_{//}\varepsilon_{\perp}}{\varepsilon_{//}\cos^2\theta + \varepsilon_{//}\sin^2\theta}, \quad (1)$$

where $\varepsilon_{//}$ and $\varepsilon_{\perp}$ are the respective permittivities for light-polarized parallel and perpendicular to the director axis $\vec{n}$. It is important to note that ε_{LC} is independent of frequency and only depends on the director axis orientation angle θ with respect to the optical wave vector k^i.

In this paper, LCs are used in the nematic phase, where the molecules float around as in the liquid phase but are still ordered in their orientation[15]. The nematic phase [11, 16] is of great interest because of the dielectric anisotropy that permits the frequency agility. "Anisotropy is then defined as the difference between parallel and perpendicular permittivities and ensues from the following relation:

$$\Delta\varepsilon_{reff} = \varepsilon_{reff//} - \varepsilon_{reff\perp}, \quad (2)$$

where $\varepsilon_{reff//}$ and $\varepsilon_{reff\perp}$ are, respectively, the parallel and perpendicular relative dielectric permittivities.

The director vector $\vec{n}$ has the same direction as the nematic LC molecules. A parallel permittivity $\varepsilon_{reff//}$ of the molecules occurs for a microwave field parallel to the director $\vec{n}$, whereas a perpendicular permittivity $\varepsilon_{reff\perp}$ is effective for a microwave field perpendicular to the director $\vec{n}$. The result of applying a sufficiently large control voltage to LC is to align the LC along the electric field due to the control voltage. This LC alignment is nearly parallel to the microwave electric field because the transmission mode of the microstrip line is quasi-TEM. On the other hand, if the control voltage is removed (changed to 0 V), the LC becomes aligned in the direction determined by the alignment layers, which is perpendicular to the microwave electric field.

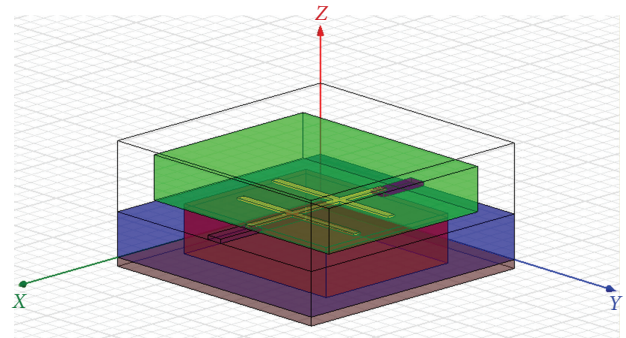

Figure 3: Structure filter DBR with an LC cavity by HFSS.

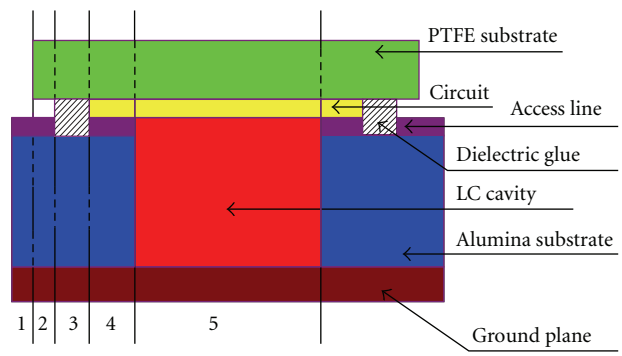

Section 1: alumina
Section 2: alumina + air + PTFE
Section 3: alumina + dielectric glue + PTFE
Section 4: alumina + PTFE
Section 5: LC + PTFE

Figure 4: Transversal cut of the filter DBR structure.

Studies over the last two decades have also conclusively demonstrated their unusually large electro- and all-optical (i.e., nonlinear-optical) response associated with the field induced director axis reorientation. These unique optical properties [17], in addition to their compatibility with almost all technologically important optoelectronic materials and their fluid nature, make them prime candidates for incorporation into nanostructured (electrically or all-optically) tunable materials/devices.

3. Synthesis and Design of the DBR Filter

3.1. Synthesis of the DBR Filter. A DBR results from the association of two different parallel bandstop structures. Each of them brings its own transmission zero with respect to its fundamental resonant condition. At the same time, their association is transparent within a given operating frequency once the bandstop structures have been properly connected under constructive recombination criteria. These result in a bandpass response created between the abovementioned lower and upper rejected bands. According to the number of available parameters and to the initial behavior of each bandstop structure, DBR allows an independent control of the following.

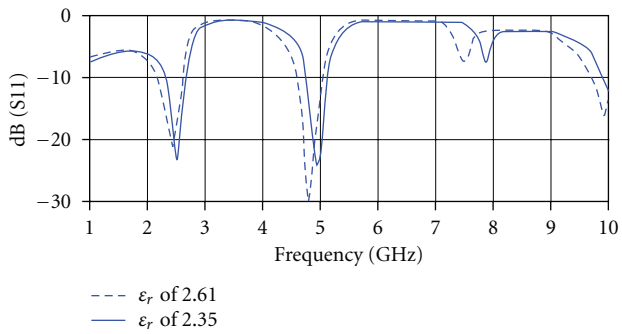

Figure 5: Simulated return losses for two different permittivities by (HFSS).

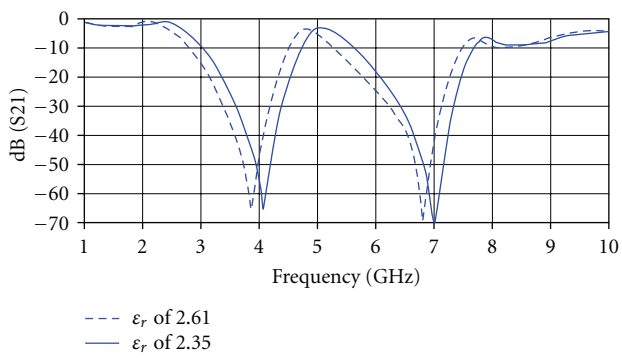

Figure 6: Simulated insertion losses for two different permittivities by (HFSS).

Thus, a DBR structure allows one to independently control [2]:

(i) one pole in the operating bandwidth;

(ii) one transmission zero in the lower attenuated band;

(iii) one transmission zero in the upper attenuated band.

Among the numerous DBR topologies available, one of the simplest ones is based on the parallel association of two open-circuited stubs of different lengths. Its easy implementation drove us to choose this topology for the design of our circuits. The inherent specifications of the filter are entered in equations called synthesis [2]. Their resolution allows one to get the electrical parameters of the lines (length, characteristic impedance).

The generic structure (see Figure 2) can be described as a parallel association of two different bandstop structures of equivalent input impedances Z_1 and Z_2. Obviously, the impedance of the whole structure is defined as in Figure 2.

This equation shows that the stub association has no incidence on the frequencies of the transmission zeros that always appear when $Z = 0$, that is, when $Z_1 = 0$ or $Z_2 = 0$. The individual incidence of each bandstop structure is then preserved. Nevertheless, a bandpass can be created when the equivalent input impedances Z_1 and Z_2 have the same modulus, but become out-of-phase. Indeed, in this case, the total impedance tends toward infinity.

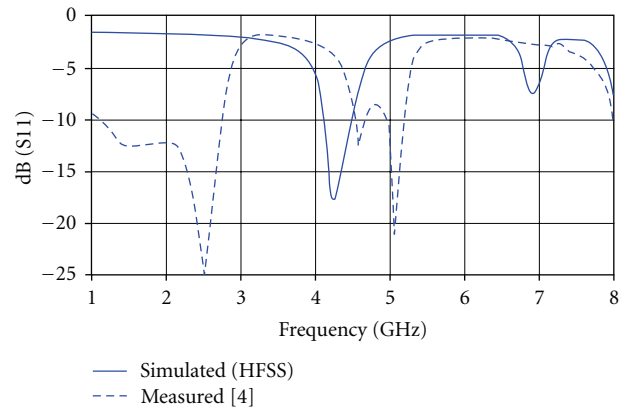

Figure 7: Simulated and measured return losses without applied DC voltage.

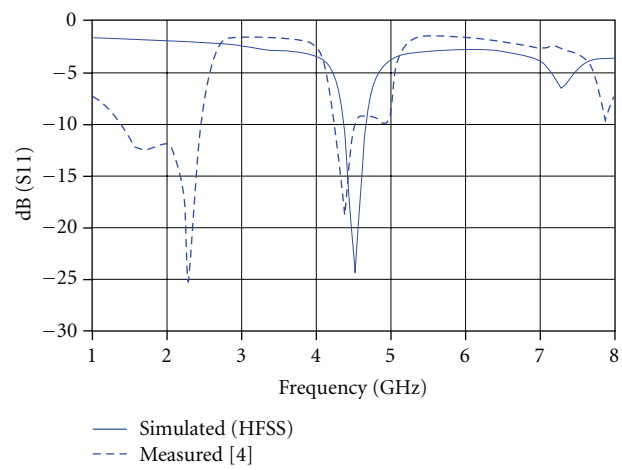

Figure 8: Simulated and measured return losses with applied DC voltage.

After modifications and optimization of the circuit, an electromagnetic calculation of the global structure is carried out with the HFSS design based on a finite element method. This method permits one to consider all of the structure elements: alumina, dielectric ink, liquid crystal, and PTFE.

3.2. Design of the DBR Filter. Figures 3 and 4 depict the designs of DBR filter, this device consist of three glued substrate in multi-levels. The bottom part made of alumina substrate $\varepsilon_r = 9.6$ and thickness = 508 μm, is composed of a cavity, where the LC is inserted by capillarity with a dielectric constant permittivity of $\varepsilon_r = 2.9$ and a loss tangent of 0.002. The upper side of the ground plane in physical contact with LC is beforehand covered with PVA and brushed with abrasive material to give an initial orientation to the LC molecules with no applied bias voltage in order to increase dielectric anisotropy. The alumina has been selected for its mechanical features (rigidity, precision to level thickness, etc.). The upper part thickness is 508 μm, who supported the motives filters, is made of Polytetrafluoroethylene (PTFE) of low permittivity ($\varepsilon_r = 2.2$). We chose this kind of material to take

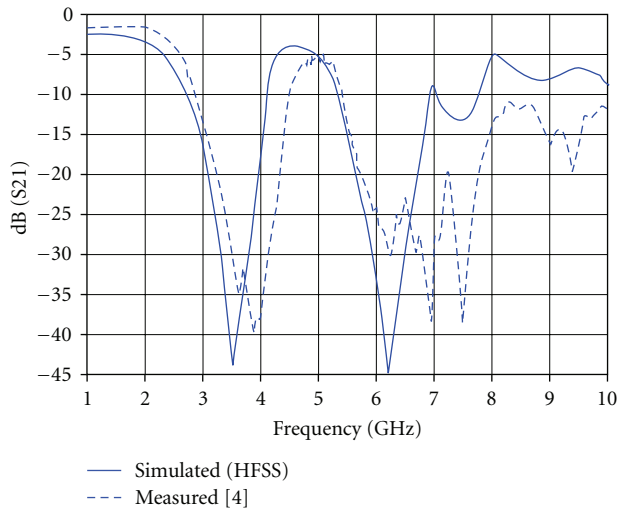

Figure 9: Simulated and measured insertion losses without applied DC voltage.

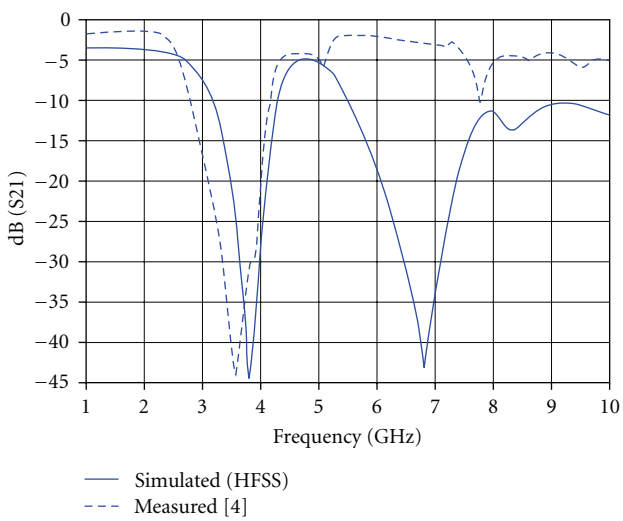

Figure 10: Simulated and measured insertion losses with applied DC voltage.

benefits of its properties; indeed, its rigidity is helpful to hold the circuit, and its low permittivity allows the concentration of field lines within the LC. Once stuck under this part, the filter is covered with PVA and brushed then in order to orient the molecules of liquid crystal mechanically and therefore to increase the dielectric anisotropy. The final assembly of the structure is made with a glued dielectric termed ink and placed so that it does not disturb the electrical response of the filter.

After its insertion in the cavity, LC is considered by the microstrip line as the main substrate; thus, its properties are modified by application of an external static electric field. As the technological process is set, we have to choose a topology filter that presents a narrow bandpass to clearly show the shift of the function. Nevertheless, we have to implement simple structure like stubs with inductive feeding to avoid the use of an anisotropic substrate model and to facilitate the bias voltage. In this way, DBR filter appears as a very good compromise. Indeed, the central frequency and the bandwidth can be tuned by only modifying lengths [1], so it can be easily controlled by permittivity variation.

4. Simulation of the DBR Filter

Figures 5 and 6 depict the results simulation return losses and insertion losses. It can be seen that the agility was obtained by varying the LC dielectric permittivity, established by dielectric characterisation, from 2.35 to 2.61.

The simulated return losses are centred around 5 GHz. The return loss achieved −20 dB from 4 to 5 GHz. The resonance frequency variation (ΔFr) is 240 MHz corresponds to a frequency agility of 4.8%. The insertion losses achieved −60 dB from 4 to 5 GHz.

Figures 7 and 8 depict the results of simulated and measured return losses with and without applied DC voltage. It can be seen that the simulated return loss achieved −15 dB from 4 to 5 GHz. The measured return loss can be seen two resonant frequencies are 2.5 GHz and 5.1 GHz.

It can be seen from Figure 8 that show the simulated return loss achieved −20 dB from 4 to 5 GHz; the measured return loss can be seen two resonant frequencies are 2.3 GHz and 4.37 GHz.

Simulations and measurement insertion losses with and without applied DC voltage show good agreement, as depicted in Figures 9 and 10. It can be seen that the simulated and measured insertion losses achieved −40 dB, respectively, −35 dB. It can be seen from Figure 10 that show the simulated and measured insertion losses achieved −40 dB.

5. Conclusion

Structure of LC-based reconfigurable tunable filter with DBR topology accordable in a band and a frequency is designed and simulated. The observation of the results confirms the potential frequency agility of the device that uses LCs. This agility was obtained by varying the LC dielectric permittivity, established by dielectric characterisation, from two different permittivities. The accuracy of simulation was verified by comparison with experimental data.

References

[1] C. Quendo, E. Rius, and C. Person, "Narrow bandpass filters using dual-behaviors resonators," *IEEE Transactions on Microwave Theory and Techniques*, vol. 51, no. 3, pp. 734–743, 2003.

[2] C. Quendo, E. Rius, and C. Person, "Narrow bandpass filters using dual-behavior resonators based on stepped-impedance stubs and different-length stubs," *IEEE Transactions on Microwave Theory and Techniques*, vol. 52, no. 3, pp. 1034–1044, 2004.

[3] E. Foum, C. Quendo, E. Rius, A. Potier et al., "Bandwdith and central frequency control on tunable bandpass filter by using MEMs cantilever," in *Proceedings of the IEEE MTT-S International Microwave Symposium*, Philadelphia, Pa, USA, 2003.

[4] J. F. Bernigaud, N. Martin, P. Laurent et al., "Liquid crystal tunable filter based on DBR topology," in *Proceedings of the*

36th European Microwave Conference (EuMC '06), pp. 368–371, Manchester, HK, September 2006.

[5] N. Martin, P. Laurent, F. Huret, and Ph. Gelin, "Influence of design liquid crystal-based devices on the agility capability," in *Proceedings of the IEEE Transactions on Microwave Theory and Techniques*, Long Beach, Calif, USA, 2005.

[6] S. Missaoui, M. Kaddour, and A. Gharbi, "Design and simulation of tunable phase shifters based on liquid crystals," *Electromagnetics*, vol. 31, no. 4, pp. 285–293, 2011.

[7] S. Missaoui, M. Kaddour, and A. Gharbi, "Development and design of multilayer antennas based on liquid crystals," *IOP Conference Series: Materials Science and Engineering*, vol. 13, no. 1, 2010.

[8] T. Kuki, H. Fujikake, and T. Nomoto, "Microwave variable delay line using dual-frequency switching-mode liquid crystal," *IEEE Transactions on Microwave Theory and Techniques*, vol. 50, no. 11, pp. 2604–2609, 2002.

[9] S. Missaoui, M. Kaddour, and A. Gharbi, "Design and simulation reconfigurable liquid crystal patch antennas on foam substrate," *Journal of Chemical Engineering and Materials Science*, vol. 2, no. 7, pp. 96–102, 2011.

[10] N. Martin, G. Prigent, P. Laurent, P. H. Gelin, and F. Huret, "Technological evolution and performances improvements of a tunable phase-shifter using liquid crystal," *Microwave and Optical Technology Letters*, vol. 43, no. 4, pp. 338–341, 2004.

[11] N. Tentillier, N. Martin, R. Douali, B. Splingart, and C. legrand, "Microwave dielectric properties of nematic liquid crystals: applications to tunable phase shifters," in *Proceedings of the 20ème International LC Conference*, Ljubljana, Slovenia, July 2004.

[12] V. Palazzari, D. Thompson, N. Papageorgiou et al., "Multiband RF and mm-wave design solutions for integrated RF functions in liquid crystal polymer system-on-package technology," in *Proceedings of the IEEE 54th Electronic Components and Technology Conference Symposium (ECTC '04)*, pp. 1658–1663, June 2004.

[13] M. M. Tentzeris, J. Laskar, J. Papapolymerou et al., "3-D-Integrated RF and millimeter-wave functions and modules using liquid crystal polymer (LCP) system-on-package technology," *IEEE Transactions on Advanced Packaging*, vol. 27, no. 2, pp. 332–340, 2004.

[14] I. C. Khoo, *Liquid Crystals, Physical Properties and Nonlinear Optical Phenomena*, John Wiley & Sons, New York, NY, USA, 1995.

[15] P. G. de Gennes, *The Physics of Liquid Crystals*, Clarendon Press, Oxford, UK, 1974.

[16] S. Singh, "Phase transitions in liquid crystals," *Physics Report*, vol. 324, no. 2–4, pp. 107–269, 2000.

[17] S. A. Jewell and J. R. Sambles, "Optical characterization of a dual-frequency hybrid aligned nematic liquid crystal cell," *Optics Express*, vol. 13, no. 7, pp. 2627–2633, 2005.